Organic & Biomolecular Chemistry

RSC Publishing

PAPER

View Article Online
View Journal

Cite this: DOI: 10.1039/c3ob25777k

Analysis of designed β-hairpin peptides: molecular conformation and packing in crystals†

Subrayashastry Aravinda,[a] Upadhyayula S. Raghavender,[a] Rajkishor Rai,[b] Veldore V. Harini,[a] Narayanaswamy Shamala*[a] and Padmanabhan Balaram*[b]

Received 23rd April 2012,
Accepted 12th April 2013

DOI: 10.1039/c3ob25777k

www.rsc.org/obc

The crystal structures of several designed peptide hairpins have been determined in order to establish features of molecular conformations and modes of aggregation in the crystals. Hairpin formation has been induced using a centrally positioned ^{D}Pro-Xxx segment (Xxx = ^{L}Pro, Aib, Ac_6c, Ala; Aib = α-aminoisobutyric acid; Ac_6c = 1-aminocyclohexane-1-carboxylic acid). Structures of the peptides Boc-Leu-Phe-Val-^{D}Pro-^{L}Pro-Leu-Phe-Val-OMe (**1**), Boc-Leu-Tyr-Val-^{D}Pro-^{L}Pro-Leu-Phe-Val-OMe (**2**, polymorphic forms labeled as **2a** and **2b**), Boc-Leu-Val-Val-^{D}Pro-^{L}Pro-Leu-Val-Val-OMe (**3**), Boc-Leu-Phe-Val-^{D}Pro-Aib-Leu-Phe-Val-OMe (**4**, polymorphic forms labeled as **4a** and **4b**), Boc-Leu-Phe-Val-^{D}Pro-Ac_6c-Leu-Phe-Val-OMe (**5**) and Boc-Leu-Phe-Val-^{D}Pro-Ala-Leu-Phe-Val-OMe (**6**) are described. All the octapeptides adopt type II′ β-turn nucleated hairpins, stabilized by three or four cross-strand intramolecular hydrogen bonds. The angle of twist between the two antiparallel strands lies in the range of −9.8° to −26.7°. A detailed analysis of packing motifs in peptide hairpin crystals is presented, revealing three broad modes of association: parallel packing, antiparallel packing and orthogonal packing. An attempt to correlate aggregation modes in solution with observed packing motifs in crystals has been made by indexing of crystal faces in the case of three of the peptide hairpins. The observed modes of hairpin aggregation may be of relevance in modeling multiple modes of association, which may provide insights into the structure of insoluble polypeptide aggregates.

Introduction

Considerable recent interest has focused on the modes of association of extended polypeptide strands (β-strands) in crystals.[1] The observed modes of association provide insights into possible structures for amyloid fibrils and polypeptide aggregates associated with a range of disease pathologies.[2] Cyclic peptide mimics have been structurally characterized and the observed packing arrangements have been correlated with the association of extended polypeptide strands in amyloid oligomers.[3] The packing motifs in crystals of acyclic peptide hairpins can also provide insights into modes of β-strand association. The crystallographic characterization of well-designed peptide β-hairpins,[4] also provides an opportunity to examine modes of aggregation of peptide molecules, which may be useful in considering models for fibrillar structures formed by insoluble segments that are of relevance in understanding the structure of amyloid deposits.[5] Constrained dipeptide templates which preferentially adopt type I′/II′ β-turn conformations have been successfully used in the design of β-hairpin structures in synthetic peptides. The type I′ and II′ β-turns are characterized by specific Ramachandran angles at the dipeptide segment (ideal values for type I′ β-turns are ϕ_{i+1} = 60°, ψ_{i+1} = 30°, ϕ_{i+2} = 90°, ψ_{i+2} = 0° and for type II′ β-turns are ϕ_{i+1} = 60°, ψ_{i+1} = −120°, ϕ_{i+2} = 90°, ψ_{i+2} = 0°).[6] These conformations may be readily imposed by the choice of residues in which the conformational options are limited. The D-Pro (^{D}Pro) residue has emerged as a unit of choice, since the covalent constraints of pyrrolidine ring formation restricts ϕ_{DPro} to values ≈+60° ± 30°.[7] The two favored regions of conformational space correspond to, ψ = +30 ± 10° and −120° ± 10°, both of which are compatible with the occurrence of ^{D}Pro at the i + 1 position of type I′/II′ β-turns.[4a] The **^{D}Pro-Xxx** segment, where any L-residue is placed at the i + 2 position, strongly favors type II′ β-turns (Fig. 1).[4a] Achiral residues like Gly and α,α-dialkylated residues (Aib and Ac_6c) facilitate the

[a]Department of Physics, Indian Institute of Science, Bangalore 560 012, India. E-mail: shamala@physics.iisc.ernet.in; Fax: +91-80-23602602; Tel: +91-80-22932856
[b]Molecular Biophysics Unit, Indian Institute of Science, Bangalore 560 012, India. E-mail: pb@mbu.iisc.ernet.in; Fax: +91-80-23600683; Tel: +91-80-22932337

†Electronic supplementary information (ESI) available: CIF files, main chain and side chain torsional angles for peptides **1–6** (Tables S1–S4), hydrogen bond parameters for **1–6** (Tables S5–S7), twist and aromatic interaction parameters for **1–6** (Tables S8 and S9). The asymmetric and packing figures for peptides **1–6** (Fig. S1–S8). ^{1}H NMR spectra of peptides **1–6** and expansion of NH region (Fig. S9–S10). CCDC 821276, 821280, 821281, 821277, 821278, 821279, 821275 and 821274. For ESI and crystallographic data in CIF or other electronic format see DOI: 10.1039/c3ob25777k

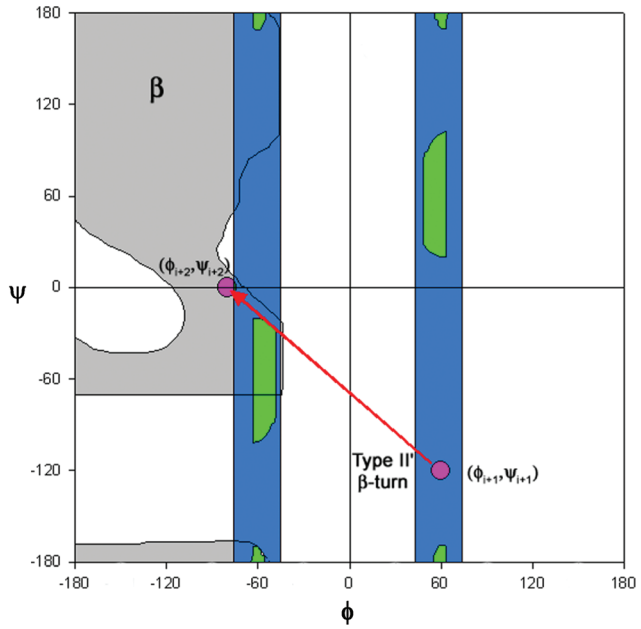

Fig. 1 Ramachandran plot showing β-sheet region (gray), conformational space accessible to Aib (green) and L-proline and D-proline (blue). The ideal conformations of residues *i* + 1 and *i* + 2 in a type II′ β-turn are indicated by a red arrow.

formation of both type I′/II′ β-turns, when used at the *i* + 2 position in ^{D}Pro-Xxx segments.[4b,8a] The type II′ β-turn in a ^{D}Pro-^{L}Pro unit was initially characterized in the crystal structure of a tripeptide.[9] Robinson's group has been instrumental in using the β-hairpin motif to design protein epitope mimetics by transplanting hairpin loop sequences from folded proteins onto hairpin-stabilizing ^{D}Pro-^{L}Pro templates.[10] In the process, they have been successful in designing and optimizing β-hairpin mimetics, which are well suited for the design of inhibitors of both protein–protein and protein–nucleic acid interactions.[11] Subsequently, the ^{D}Pro-^{L}Pro segment has been used in nucleating hairpin structures in synthetic antigenic peptides.[12] In particular, β-hairpin shaped peptidomimetics based on the membranolytic host-defense peptide protegrin I containing loop sequences linked to a ^{D}Pro-^{L}Pro template stabilizing the hairpin conformations have been shown to possess potent antimicrobial activity in a mouse septicemia infection model.[13] Peptide hairpins have also been developed as novel biomaterials, especially in the rational design of amphiphilic sequences which can form functionally useful hydrogels.[14] We have been systematically studying the conformational properties of synthetic oligopeptides containing centrally positioned ^{D}Pro-^{L}Pro segments in order to unambiguously establish the conformational properties of potential hairpin peptides. The NMR structural characterization of a β-hairpin in the synthetic peptide, Boc-Leu-Phe-Val-**^{D}Pro-^{L}Pro**-Leu-Phe-Val-OMe, has been reported.[15]

The ability of α,α-dialkylated residues, of which the Aib residue is the prototype, to be restricted to local helical regions (right-handed α-helix, α_R: (ϕ, ψ) = (−60°, −30°) and left-handed α-helix, α_L: (ϕ, ψ) = (60°, 30°) is well established.[16] This conformational preference may be exploited to construct prime turns for β-hairpin nucleation in ^{D}Pro-Aib (type II′ β-turn)[4b] and Aib-^{D}Xxx (type I′ β-turn)[17] segments. The recent crystal structure of an octapeptide, Boc-Leu-Val-Val-**Aib-^{D}Pro**-Leu-Val-Val-OMe, illustrates an example of a type I′ β-turn nucleated hairpin (Boc: *tert*-butoxycarbonyl, OMe: methyl ester).[18] As part of an ongoing project aimed at the synthetic and structural characterization of peptide β-hairpins and multi-stranded β-sheets, we describe in this report hairpin conformations in crystals of the following model peptide sequences incorporating central ^{D}Pro-^{L}Pro and ^{D}Pro-Xxx segments (where Xxx is Ala, Aib and Ac_6c). Boc-Leu-Phe-Val-^{D}Pro-^{L}Pro-Leu-Phe-Val-OMe (**1**), Boc-Leu-Tyr-Val-^{D}Pro-^{L}Pro-Leu-Phe-Val-OMe (**2**, polymorphic forms labeled as **2a** and **2b**), Boc-Leu-Val-Val-^{D}Pro-^{L}Pro-Leu-Val-Val-OMe (**3**), Boc-Leu-Phe-Val-^{D}Pro-Aib-Leu-Phe-Val-OMe (**4**, polymorphic forms labeled as **4a** and **4b**), Boc-Leu-Phe-Val-^{D}Pro-Ac_6c-Leu-Phe-Val-OMe (**5**) and Boc-Leu-Phe-Val-^{D}Pro-Ala-Leu-Phe-Val-OMe (**6**). A detailed consideration of the observed packing motifs is presented, providing insights into the modes of aggregation of antiparallel β-strand structures.

Results and discussion

Structures of β-hairpins

Crystals of peptides **1–6** consist of two molecules in the asymmetric unit. All molecules adopt type II′ β-turn nucleated, β-hairpin conformations. The turn segment in peptides **1–3** is ^{D}Pro-Pro and in peptides **4** to **6**, ^{D}Pro-Xxx (where Xxx is Aib(**4**), Ac_6c(**5**) and Ala(**6**)) (Fig. 2). The individual hairpins of the peptides **1–6** (16 independent octapeptide molecules) adopt very similar backbone conformations, as indicated by the superposition of the backbone atoms (N, C^{α}, C) of the residues 2–7 (r.m.s.d. of 0.132 Å, Fig. 3). Residues 1–3 and 6–8 adopt conformations corresponding to β-strands, whereas residues 4–5 occur in the conventional type II′ β-turn conformation, with the exception of molecule A in peptide **6**. Main chain and side chain torsional angles are summarized in the ESI Tables S1–S4.† A scatter plot of backbone torsional angles for all 8 residues in the various β-hairpin structures is shown in Fig. 4. While most residues are fairly tightly clustered in ϕ, ψ space, significant variation is observed for the C-terminus Val residue. Fraying of the inter-strand hydrogen bonds at the hairpin terminus is a common feature. Three intramolecular hydrogen bonds are observed to stabilize the β-hairpin conformation in all the individual molecules, with four hydrogen bonds being observed only in the case of peptide **6** (molecule A). The individual molecules are stabilized by three cross-strand hydrogen bonds (N13···O16, N16···O13, and N18···O11) and (N23···O26, N26···O23, and N28···O21 (ESI Tables S5–S7†). Residue 5 in molecule A, peptide **6** (^{D}Pro(4)-Ala(5)) is a Ramachandran outlier, with backbone torsion angles (ϕ = −138.3°, ψ = −13.8°) lying clearly in the disallowed region (Fig. 4). Inspection of the turn segment reveals this is the only case where the ^{D}Pro(4) residue adopts ϕ, ψ values (ϕ = 84.6°, ψ =

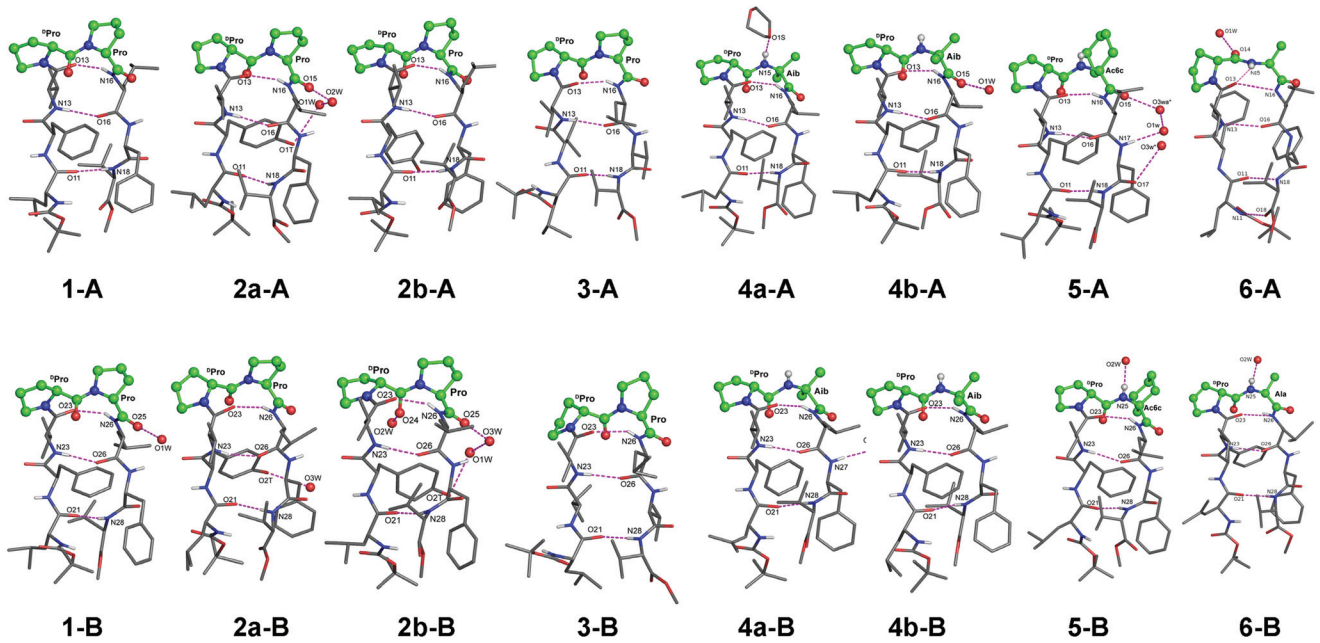

Fig. 2 Individual molecular conformations of the peptides **1–6**. Top panel shows molecule A and bottom panel shows molecule B. The turn region is shown in ball-and-stick (green) and the cocrystallized water molecules as spheres (red).

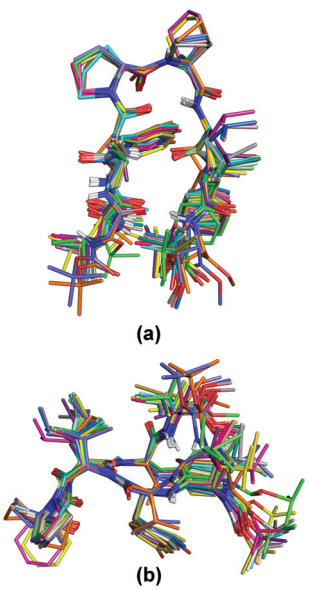

Fig. 3 (a) Superposition of the backbone atoms (N, C^{α}, C) of the individual β-hairpin molecules of the peptides **1–6** (RMSD = 0.132 Å). Carbon atoms are colored differently for each molecule, whereas nitrogen and oxygen atoms are colored blue and red, respectively. (b) Side view of the β-hairpin molecules.

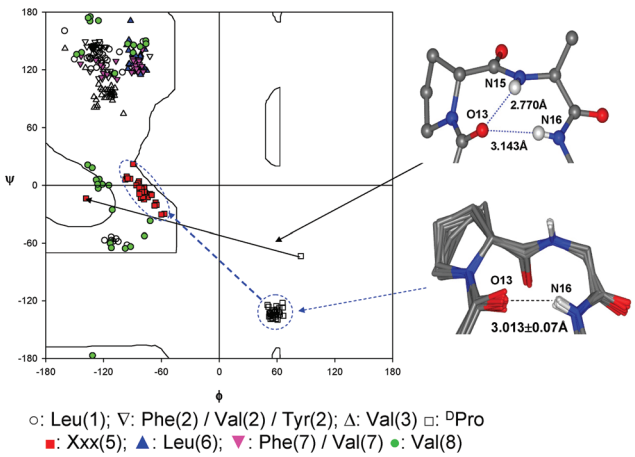

Fig. 4 Distribution of backbone torsion angles (ϕ, ψ) in peptide hairpins represented on a Ramachandran map. Data from 18 peptide structures, corresponding to 32 independent hairpin molecules. The superposition of the type II′ β-turn segment in 31 molecules (RMSD = 0.104 Å; Val(3)CO···NHLeu(6) = 3.01 ± 0.07 Å) is shown. The distorted turn segment in peptide **6** molecule A is shown separately. Backbone torsion angles at DPro(4) and Ala(5) in **6** deviate considerably from the clusters observed in the other 31 examples. The hydrogen bond distances are Val(3)CO···NHAla(5) = 2.770 Å and Val(3)CO···NHLeu(6)NH = 3.143 Å. The Val(3)CO···NHXxx(5) distances in the other 31 examples are 3.22 ± 0.09 Å.

−73.5°) corresponding to a classical γ-turn structure,[19] stabilized by a 3 → 1 hydrogen bond between the Val(3)CO and Ala(5)NH group (N···O = 2.77 Å, H···O = 2.08 Å and ∠N–H···O = 136.8°). In peptide **6** molecule A, the turn segment is significantly distorted from an ideal type II′ structure, with Val(3) CO potentially accepting two simultaneous hydrogen bonds (3 → 1,4 → 1). Interestingly, the two antiparallel strands are perfectly registered with all four inter-strand hydrogen bonds being formed. Torsional strain at the Ala(5) residue in peptide **6** molecule A must undoubtedly be compensated by energetically favorable interactions, both intramolecular and intermolecular. The twist of the individual hairpin molecules is evaluated as a virtual torsion angle between C^{α} atoms of residues 3–6 (ESI Table S8†). The twist of the individual hairpins in all the hairpin structures is right-handed and is observed to

be in the range −10° to −20°. Molecule B in peptide **6** is slightly more twisted than the other individual molecules in the series (−26.7°).

Side chain conformation and interactions

By convention, the signs of χ^1, χ^2, χ^3 and χ^4 torsions decide the C^γ-*exo* (UP) and C^γ-*endo* (DOWN) pucker of the pyrrolidine ring (−, +, −, +corresponding to C^γ-*exo* (UP) and +, −, +, − corresponding to C^γ-*endo* (DOWN)).[20] Accordingly, the ^{D}Pro(4) residue is observed to adopt a C^γ-*endo* (DOWN) pucker in **1**, **2a**, **3** (molecule A) **4a**, **4b** and **5**. C^γ-*exo* (UP) puckering is observed for the ^{D}Pro(4) in **3** (molecule B) and **6**. The Pro(5) residue adopts a C^γ-*endo* (DOWN) in **1**, **2a**, **2b**, and **3** (molecule A) and C^γ-*exo* (UP) in **3** (molecule B). Aromatic–aromatic interactions[17,21] are observed between the Phe residues present on the antiparallel strands of all the peptides except peptide **3**, where the strands did not have Phe residues. The interaction parameters for the π···π interactions are mostly T-shaped or inclined (ESI Table S9†). Notably, in peptide **6** molecule A, the aromatic sidechains Phe(2) and Phe(7) adopt different backbone conformations as compared to all other peptides containing a facing pair of phenyl rings at this non-hydrogen bonding site in the β-hairpins. It is observed that the Phe residues, in the case of peptide **6**, are involved in a network of interactions across symmetry-related molecules, as discussed subsequently.

Packing of the β-hairpins in crystals

In crystals the two molecules in the asymmetric unit, of all the peptides **1–6**, are inclined (approximately) orthogonally with respect to each other. The angle between the two molecules in the asymmetric unit is calculated by fitting a mean plane passing through the C^α atoms of the residues 2–7 of the individual molecules (ESI Table S8†). The two molecules in the asymmetric unit are inclined to each other at an angle of ∼52° to ∼77°, with the exception of peptide **3**, where an approximate parallel orientation of the molecules is observed (∼37°). Peptide **6** shows an almost perfect orthogonal arrangement with the angle of inclination being ∼86° (ESI Fig. S1†). Two strong intermolecular hydrogen bonds (N12···O22 and N22···O12) are observed connecting the two molecules in the asymmetric unit in all the peptides (ESI Tables S5–S7†). Hydrogen bonds (intramolecular and intermolecular), involving peptide backbone NH and CO groups, stabilize the packing of the molecules in the plane of the sheet. Packing of the molecules perpendicular to the plane of the sheet is mediated by peptide–solvent hydrogen bonds. Cocrystallized solvent molecules help in stabilizing the molecular conformation by forming hydrogen bonds with the peptide backbone. The cocrystallized solvents in **1**, **2a**, **2b**, **4a**, **4b**, **5** and **6** are observed to be involved in bridging the symmetry related molecules along the direction of the intramolecular and intermolecular hydrogen bonds. The structure of peptide **3** is devoid of solvent, leading to increased interpeptide hydrogen bonding between the symmetry related molecules. This is the only example of a β-hairpin crystal structure with no cocrystallized solvent in the asymmetric unit. The ^{D}Pro-Pro segment in the peptides **1**, **2a**, **2b** and **3** is not solvated, presumably because of the lack of free NH groups.

Boc-Leu-Phe-Val-^{D}Pro-^{L}Pro-Leu-Phe-Val-OMe (1). The lone water molecule, cocrystallized with the peptide molecule in the asymmetric unit, helps in bridging the molecules related by the translation symmetry (O1w (x, y, z) and N17 (x, y + 1, z) and O15 (x, y + 1, z)) by the formation of hydrogen bonds (ESI Table S5 and Fig. S2†).

Boc-Leu-Tyr-Val-^{D}Pro-^{L}Pro-Leu-Phe-Val-OMe (2a and 2b). In both the polymorphic crystal forms, three fully occupied, co-crystallized water molecules are observed in the asymmetric unit. The water molecules co-crystallized with the peptide in **2a**, help in bridging symmetry related molecules by hydrogen bonds (O2w(x + 1, y, z) and O15(x, y, z), O2w(x, y, z) and N27(x, y, z)) and also interact with the hydroxyl group of the Tyr residue (O1w(x, y, z) and O1t(x, y, z), O3w(x, y, z) and O2t(x, y, z)). In contrast, in **2b** the co-crystallized water molecules are observed to form peptide backbone hydrogen bonds with the molecule-B (O2w(x, y, z)···O24(x, y, z) and O1w(x, y, z)···O25(x, y, z)) and with the Tyr(2) OH (O3w(x, y, z)···O1t(x, y, z)). O1w and O3w also form water–water hydrogen bonds. O1w is observed to hold the translationally related molecules by hydrogen bonds (O1w(x, y, z)···O25(x, 1 + y, z)), whereas O2w water molecule is observed to bridge 2_1 screw related peptide molecules (O2w(x, y, z)···O1t(−x, y + 1/2, 1 − z)) in a direction perpendicular to the propagation of β-sheet hydrogen bonds (approximately along the *b*-axis) as opposed to peptide **1**. The turn segment is not hydrated in both the independent molecules in the case of **2a**, whereas in **2b** molecule-B shows a strong peptide–water hydrogen bond with the backbone carbonyl oxygen of the turn segment (O2w(x, y, z)···O24(x, y, z)), which in turn forms a hydrogen bond with peptide molecule (ESI Table S5 and Fig. S3†).

Boc-Leu-Val-Val-^{D}Pro-^{L}Pro-Leu-Val-Val-OMe (3). The two molecules in the unit cell of peptide **3** pack as two independent and separate β-sheets. The packing of the individual molecules, along the crystallographic *a*-axis, is stabilized by the formation of three intermolecular peptide–peptide hydrogen bonds (ESI Table S6†). A bifurcated hydrogen bond is observed at the N-terminus of both the molecules (N11(x, y, z) and O17(1 + x, y, z), N12(x, y, z) and O17(1 + x, y, z), N21(x, y, z) and O27(−1 + x, y, z), N22(x, y, z) and O27(−1 + x, y, z)). This brings the N-terminus of one β-hairpin molecule in register with the C-terminus of the next translated molecule. The overall packing in the crystals can be described as corresponding to that of the "parallel" β-sheet (ESI Fig. S4†).

Boc-Leu-Phe-Val-^{D}Pro-Aib-Leu-Phe-Val-OMe (4a and 4b). The octapeptide **4a** crystallized with two molecules in the asymmetric unit and a cocrystallized dioxane and a water molecule.[2] In the crystals, the dioxane molecule helps in bridging the peptide molecules related by symmetry with hydrogen bonds (O2S(x, y, z) and N25(−1 + x, y, z)) (ESI Table S6†). The water molecule is involved in bridging the translated molecules (O2w (x, y, z) and O15(1 + x, y, 1 + z)).

In peptides **1–3** the design of the β-turn using the L-Pro residue at the $i + 2$ position precludes any solvation at the central peptide unit of the turn region. In contrast the β-turn in **4a** reveals solvation of the central ^{D}Pro-Aib peptide unit. This is a common feature in β-turns observed in protein structures.[22] In contrast, **4b** was observed to have a single water molecule in the asymmetric unit. The cocrystallized water in **4b** is seen to be involved in bridging translated molecules by hydrogen bonding with the peptide backbone (O1w(x, y, z)···O15(x, y, z), and O1w(x, y, z)···N27($-1 + x$, y, $-1 + z$)). One intermolecular hydrogen bond between the translated molecules is also observed to be involved in stabilizing the packing of the molecules (O27(x, y, z)···N27($1 + x$, y, $1 + z$)) (ESI Table S6†). In **4b** unlike **4a**, there is no stabilizing interaction mediated by solvent, in a direction perpendicular to the β-sheet hydrogen bonds. It can be deduced that the packing of the molecules is very robust in both the crystal forms and the cocrystallized solvents occupy the void space in the crystals, effectively stabilizing the packing by getting involved in favorable hydrogen bonding interactions with the peptide backbone. It is likely that the dioxane molecules might have escaped from the crystals over the long period of storage. The symmetry related layers of the peptide molecules in **4b** retain all the characteristics of molecular packing and hydrogen bonds, despite the absence of the bridging solvent mediated hydrogen bond, connecting the screw-related layers as in **4a**. This feature is concomitant with shrinkage in the unit cell axis corresponding to the dimension of the dioxane molecule and a slight rearrangement of the symmetry-related molecules, with denser packing along a direction perpendicular to the β-sheet (ESI Fig. S5†).

Boc-Leu-Phe-Val-^{D}Pro-Ac$_6$c-Leu-Phe-Val-OMe (5). The asymmetric unit of **5** contains three cocrystallized water molecules, of which one is disordered (the water molecule O3w is disordered over two positions O3w and O3wa, with occupancies of 0.42 and 0.58). These three water molecules act as intermolecular solvent bridges in the orthorhombic form **5**, as compared to the water and dioxane molecules in the monoclinic form.[8a] Three water molecules bridge free CO and NH groups in the neighboring symmetry related molecules, forming a complex network of intermolecular hydrogen bonds, stabilizing the packing in crystals. O1w and O3w link adjacent molecules related by translational symmetry along the crystallographic *a*-axis direction *via* the strand segment. The asymmetric units are linked along [1 0 0] direction, by a direct interpeptide hydrogen bond N27···O17($x + 1$, y, z) and three water bridges, involving N17···O1w···O25($x - 1$, y, z), O17···O3w*···O25($x - 1$, y, z) and O15···O3wa*···O1w···O25($x - 1$, y, z), respectively (ESI Table S7†). The distance between O3w* and O1w is 2.02 Å, whereas it is 4.748 Å between O3w* and O3wa* (* indicates two disordered positions of the water molecule O3w). Along the crystallographic *b*-axis, the central peptide NH (Ac$_6$c,NH) of molecule-B is hydrogen bonded to water molecule O2w, which is further anchored by two hydrogen bonds to O18 and O27 of symmetry related molecules (O2w···O18($-x + 1$, $y + 1/2$, $-z + 1/2$), O2w···O27($-x + 2$, $y + 1/2$, $-z + 1/2$)). The terminal methoxy ester group of molecule-B is also oriented such that it is also involved in hydrogen bond with O2w (O2w···O28($-x + 2$, $y + 1/2$, $-z + 1/2$)). The 1,1 disubstituted cyclohexane rings of the Ac$_6$c residues, in both the polymorphic forms of **5**, adopt almost ideal chair conformations, the amino group occupying an axial position[8] (ESI Fig. S6†).

Boc-Leu-Phe-Val-^{D}Pro-Ala-Leu-Phe-Val-OMe (6). Peptide **6** crystallized in the orthorhombic space group $P2_12_12_1$, with two peptide molecules and two water molecules in the asymmetric unit, whereas the polymorphic form (also $P2_12_12_1$) previously described crystallized with two peptide molecules, one isopropanol and three water molecules in the asymmetric unit.[4b] The crystals of the polymorphic form were obtained by slow evaporation from a mixture of isopropanol–water, whereas the crystals of **6** were grown from dimethylformamide (DMF) to which small amount of water was added. In both the cases thin needles were formed. The puckering of the ^{D}Pro(4) residue is different in both the forms. The ^{D}Pro(4) residue is C$^{\gamma}$-*exo* (UP) puckered in **6** and C$^{\gamma}$-*endo* (DOWN) in the polymorphic form (molecule-A). Peptide **6** has the two molecules oriented at approximately 86°. The molecule-A is observed to form all the four possible intramolecular cross-strand hydrogen bonds for an octapeptide hairpin (N11···O18, N13···O16, N16···O13 and N18···O11), whereas molecule-B is observed to form only three cross-strand intramolecular hydrogen bonds (N23···O26, N26···O23 and N28···O21) (ESI Table S7†). Cocrystallized water molecules are observed to form hydrogen bonds with the backbone atoms, ^{D}Pro(4) CO in molecule-A (O1w···O14) and Ala(5) NH in molecule-B (O2w···N15), of the β-turn segment. Three peptide–peptide backbone cross-strand intermolecular hydrogen bonds stabilize packing along the *a*-axis (N12···O22, O12···N22, O17···N27). The adjacent hairpins are also connected by solvent mediated peptide–water hydrogen bonds (O1w(x, y, z)···N17($1/2 + x$, $3/2 - y$, $2 - z$), O1w(x, y, z)···O15($1/2 + x$, $3/2 - y$, $2 - z$), O2w(x, y, z)···O27($-x$, $1/2 + y$, $3/2 - z$)). In contrast, in the polymorphic form the two molecules in the asymmetric unit are oriented at an angle of approximately 67° with respect to each other. Extended packing of this asymmetric unit is achieved through a complex intermolecular hydrogen bonding pattern, involving two bridging water molecules, O1w and O2w. O2w is also involved in association of molecule-A and its symmetry-related neighbors along the *b*-axis. A third water molecule, O3w, forms hydrogen-bonded bridges along the *c*-direction between Ala(5) NH and Val(8) CO of symmetry related molecule-B. The lone isopropanol molecule appears to fill cavities and is hydrogen bonded only to O3w[4b] (ESI Fig. S7†). It is observed that the π···π interactions extend beyond being restricted to the individual molecules in the case of peptide **6**. The Phe(2) residue of molecule-A in **6** is involved in two additional T-shaped aromatic interactions with one translated molecule (x, $1 + y$, z)(R_{cen} = 6.617 Å, R_{clo} = 4.637 Å, γ = 51.06°) and one symmetry related molecule ($-x$, $y + 1/2$, $-z$) (R_{cen} = 6.437 Å, R_{clo} = 4.220 Å, γ = 52.82°). (R_{cen}: centroid–centroid distance, R_{clo}: shortest distance between two carbon atoms of the interacting rings and γ: interplanar

angle). In turn, the Phe(2) of molecule-B is involved in a weaker π···π interaction with a 2_1-screw symmetry related molecule-A (R_{cen} = 7.155 Å, R_{clo} = 5.083 Å, γ = 72.56°). All of the above weakly polar, π···π interactions observed in the structure of **6** are a result of the unusual orientation (completely orthogonal) of the molecules in the asymmetric unit. As already noted molecule-A has all its backbone cross-strand intramolecular hydrogen bonds satisfied. A ladder of aromatic interactions appears to be involved in the further stabilization of the packing of the molecules in the crystals of peptide **6** (ESI Fig. S8†).

Indexing of crystal faces and insights into the growth of crystalline plates of β-hairpins

Aggregation of molecules in solution to form nuclei that grow along specific directions must precede the formation of single crystals. Nucleation and crystal growth are poorly understood phenomena, at a molecular level. In the case of peptides the development of the principles for the design of sequences that facilitate crystal formation is not readily achieved. In the case of conformationally restricted peptides, considerable success has been realized in the crystallization of hydrophobic helical sequences.[4a,16f–h,23] Attempts to correlate observed crystal symmetries with models for nucleation and growth have been reported.[24] Hydrophobic β-hairpins have been more recalcitrant to crystallization, often yielding thin, two-dimensional plates. This morphology suggests that while aggregate formation in two dimensions is facile, presumably mediated by antiparallel β-strand hydrogen bonds, ordered packing along the third dimension is less favored. To test this hypothesis, face indexing of selected peptide β-hairpin crystals has been carried out.

Boc-Leu-Phe-Val-^{D}Pro-^{L}-Pro-Leu-Phe-Val-OMe (1). The plate like single crystal on which the diffraction data was collected had the macroscopic dimensions of 0.80 × 0.12 × 0.01 mm. It is clear that two dimensions, length and breadth, correspond to the well developed faces of the crystal. The peptide crystallized in the monoclinic space group $P2_1$, with two molecules in the asymmetric unit. The cell parameters of the crystal are a = 14.403 Å, b = 18.932 Å, c = 25.490 Å and β = 105.67°. Indexing of the faces reveals that the (010) plane corresponds to the b-axis (18.962 Å); it is collinear with the length of the crystal (0.80 mm). All the intramolecular and intermolecular hydrogen bonds are formed along the b-axis. The cocrystallized water molecule also forms hydrogen bonds along the b-axis. The (100) plane could be indexed to the a-axis (14.403 Å), which is along the thickness of the crystal (0.01 mm). The (001) planes could be indexed to the c-axis (25.490 Å); it is collinear with the breadth of the crystal (0.12 mm). The two molecules in the asymmetric unit are inclined to each other at an angle of ≈60°. Molecule A is oriented, with its extended strands approximately along the a-axis, while the strands in molecule B lie along the c-axis. Fig. 5 shows the projection of the molecules along the bc-plane, corresponding to the [100] direction. The two layers of molecules shown are related by a 2_1 screw. It can be seen

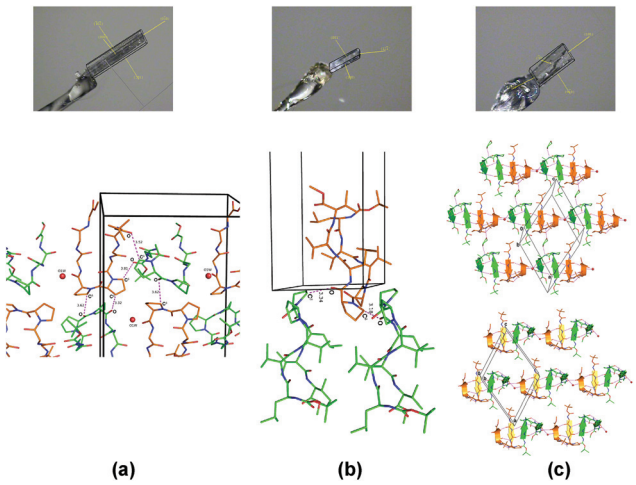

Fig. 5 Indexing of the crystal faces of peptides (a) **1**, (b) **3** and (c) **4b**. Top panel shows the crystal with the macroscopic faces indexed and the planes indicated as yellow lines with the direction indicated. Bottom panel shows the weak interactions in the peptides for peptides **1** and **3**. The direction of escape of solvent dioxane molecules in the polymorphic forms of peptide **4** is coincident with the length of the crystal.

that β-turn segments approach each other in the symmetry related layers. The ^{D}Pro-Pro segment is not hydrated in both the molecules. The only possible weak interaction is that of $C^{\delta}H\cdots O$ type involving the Pro residues.[25] A close-up view of the weak interactions observed in the turn segment provides clues to the growth of the crystal faces (Fig. 5). It is clear that, apart from hydrogen bonding, which is the stabilizing interaction along the b-axis, weak interactions of the CH···O type may contribute to the packing along the c-axis. The preferential growth of the crystal along the b and c direction may arise from these contributing factors. On the other hand, the interactions along the perpendicular direction that is along the a-axis, are purely apolar (van der Waals), corresponding to the weak interactions of the projecting side chains of the strand residues; consequently growth along this face is significantly slower.

Boc-Leu-Val-Val-^{D}Pro-^{L}Pro-Leu-Val-Val-OMe (3). The crystals of **3** were assigned to the triclinic space group $P1$ with two molecules in the asymmetric unit. All the crystals were found to be needles. The single crystal on which the diffraction data was collected had the macroscopic dimensions of 0.49 × 0.09 × 0.05 mm. The cell parameters of the crystal are a = 9.922 Å, b = 11.229 Å, c = 26.423 Å and α = 87.15°, β = 89.44°, γ = 73.28°. Two of the macroscopic faces could be indexed, corresponding to the two crystallographic axes. The (100) plane corresponds to the breadth (0.09 mm) of the crystal and is aligned along the a-axis (9.922 Å). The (001) plane corresponds to the crystallographic c-axis (26.423 Å) and is observed to be collinear with thickness of the crystal (0.05 mm). The length of the crystal (0.49 mm) could be indexed to correspond to the (121) and (121) planes. Molecules are approximately oriented along the (121) planes and the set of intra- and intermolecular hydrogen bonds propagate along the planes (Fig. 5). This can be taken

approximately along the *bc*-plane. There are no free NH groups in the crystal structure, as all the amide nitrogen atoms are involved in hydrogen bonds. The two molecules form separate β-sheets. There is no cocrystallized solvent in the structure and the molecules are packed in parallel fashion in the crystals. The orientation of the molecules in the adjacent asymmetric units and the interactions between them would decide the growth along (100) and (001) planes. The molecules in the adjacent asymmetric units, along the *ab*-plane or (001) plane are oriented with their β-turn segments, ^{D}Pro-Pro, overlapping with each other. $C^{\delta}H\cdots O$ hydrogen bonds, involving the Pro residues, appear to be stabilizing interactions in this direction, perpendicular to the hydrogen bond direction. The interactions in the asymmetric unit are between the termini of the hairpins, *tert*-butoxycarbonyl (Boc) and methyl ester groups (OMe), with the two molecules oriented with their termini facing each other. The interactions along the *b*-axis or (010) planes are essentially apolar, involving the projecting side chains of the β-strand residues.

Boc-Leu-Phe-Val-^{D}Pro-Aib-Leu-Phe-Val-OMe (4b). The habit of the crystal of **4b** can be classified as 'platy'. The dimensions of the crystal used for collecting X-ray diffraction data are 0.40 × 0.20 × 0.04 mm. The cell parameters obtained were a = 18.095 Å, b = 23.032 Å, c = 18.637 Å and β = 117.47°. The peptide crystallized in the monoclinic space group $P2_1$, with two molecules in the asymmetric unit oriented orthogonally (~60°) to each other. The (100) plane, *a*-axis (14.318 Å), was indexed along the length of the crystal (0.40 mm). This corresponds to the direction of hydrogen bonding, intra- and intermolecular, in the crystals. The (010) plane, *b*-axis (18.992 Å), was indexed along the breadth of the crystal (0.20 mm). The (101) plane was indexed along the thin dimension of the crystal (0.04 mm). The polymorphic form (**4a**) of the above crystal has the following cell parameters a = 18.41 Å, b = 23.22 Å, c = 19.24 Å and β = 118.04°. Noticeable differences can be seen in the cell dimensions of the *a*- and *c*-axes. The cocrystallized dioxane molecule observed in **4a** is not present in **4b**. The crystal used in the structure solution and refinement of the sequence **4a** was observed to be no longer transparent. It can be seen that the dioxane molecules in the structure of **4a** lie on the (200) plane. The (200) plane is along the length of the crystal of **4b**, hence it is possible that dioxane molecules could have escaped from the crystal after a prolonged time, concomitant with a corresponding reduction in the *a*-axis by 0.315 Å (Fig. 5), corresponding to a decrease in the volume of ~369 Å^3.

Classification of peptide β-hairpins based on their self-assembly in crystals

Broadly, peptide β-hairpins can be classified into three types based on the way in which the individual peptide molecules associate with each other in crystals. The three classes correspond to (i) parallel packing, (ii) anti-parallel packing, and (iii) orthogonal packing. Though the individual β-strands of the β-hairpins are antiparallel in all the three cases, it is the local association of the molecules with the nearest neighbors which forms the basis for the classification, as illustrated schematically in (Fig. 6). Representative examples are chosen to highlight the gross features of packing arrangements. Parallel packing corresponds to a peptide molecule being in register with a symmetry related, translated molecule. This is the simplest type of packing and is observed in all the sequences crystallizing in the triclinic space group $P1$. The other example is where the two peptide molecules associate adjacently, with the edge of one hairpin in register with the β-turn segment of the next hairpin. This is observed in only one β-hairpin, the decapeptide Boc-Met-Leu-Phe-Val-^{D}Pro-Ala-Leu-Val-Val-Phe-OMe[4b] (space group $P1$). Both the parallel and antiparallel packing arrangements are observed in the triclinic space group $P1$. The "orthogonal" packing is a special case, wherein the two peptide molecules associate through β-sheet like hydrogen bonds at an angle with respect to each other (~60°). This arrangement is unusual, in the sense of packing of molecules, in the asymmetric unit. Multiple molecules in the asymmetric unit are usually observed to possess non-crystallographic symmetry. In all the cases, where multiple molecules were observed in the asymmetric unit (Z' > 1) a pseudo 2-fold axis is invariably observed. Grossly, it lies in the middle of the interpeptide intermolecular cross-strand hydrogen bonds and more or less collinear with a crystallographic two fold axis. β-hairpin peptide sequences containing all α-amino residues and possessing Leu-Phe-Val as β-strand segments have been, without exception, observed to be orthogonally packed, and usually crystallize in space groups which possess a 2_1 screw. Table 1 provides a summary of the β-hairpin crystal structures available in the literature and those presented here and their classification based on the packing of the molecules observed in the solid state.

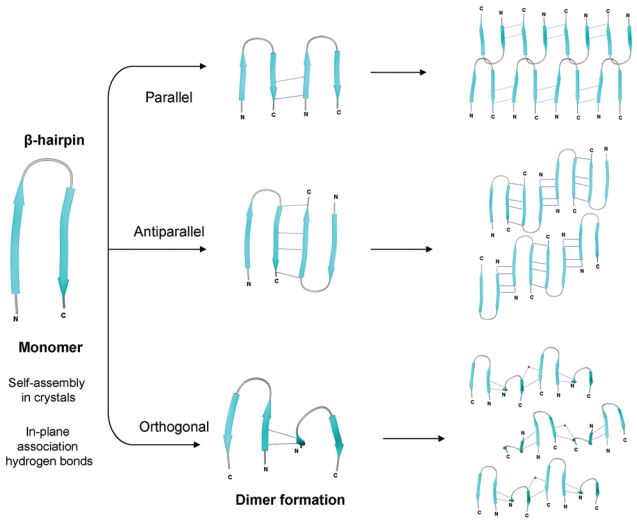

Fig. 6 Schematic illustration of the packing of β-hairpin molecules in crystals. Monomers can self-assemble into dimers in three different ways. Further assembly into tetramers is a consequence of space group symmetry, non-crystallographic symmetry, hydrophobic interactions and weak interactions. Interactions in the plane of the sheets are invariably hydrogen bonds, whereas the interactions in perpendicular directions are weak and hydrophobic in nature.

Table 1 Classification of β-hairpin peptide crystal structures

No.	Sequence	Space group	Z/Z'[a]	β-turn	Cocrystallized solvent	Packing in crystals	Reference
1	Boc-Leu-Val-Val-**^{D}Pro-Gly**-Leu-Val-Val-OMe. a = 9.739 Å, b = 11.579 Å, c = 26.253 Å, α = 98.39°, β = 120.44°, γ = 107.80°	$P1$	2/2	Type II′	2 H_2O	Parallel	29*a*
2	Boc-Leu-Val-Val-**^{D}Pro-Ala**-Leu-Val-Val-OMe. a = 9.942 Å, b = 11.240 Å, c = 25.882 Å, α = 86.14°, β = 95.62°, γ = 104.72°	$P1$	2/2	Type II′	1 H_2O	Parallel	29*b*
3	Boc-Leu-Val-βPhe-Val-**^{D}Pro-Gly**-Leu-βPhe-Val-Val-OMe. a = 19.059 Å, b = 19.470 Å, c = 21.077 Å	$P2_12_12_1$	4/2	Type I′	3 H_2O	Antiparallel	29*c*
4	Boc-βPhe-βPhe-**^{D}Pro-Gly**-βPhe-βPhe-OMe. a = 9.854 Å, b = 10.643 Å, c = 25.296 Å, β = 100.39°	$P2_1$	2/1	Type II′	1 CH_3OH	Parallel	29*d*
5	Boc-Leu-Phe-Val-**Aib-^{D}Ala**-Leu-Phe-Val-OMe. a = 10.004 Å, b = 13.724 Å, c = 51.214 Å	$P2_12_12_1$	4/1	Type I′	4 H_2O	Parallel	17
6	Boc-Leu-Val-βVal-**^{D}Pro-Gly**-βLeu-Val-Val-OMe. a = 34.184 Å, b = 10.673 Å, c = 18.965 Å, β = 120.44°	$C2$	4/1	Type I′	1 H_2O	Antiparallel	29*e*
7	Boc-Leu-Val-Val-**^{D}Pro-Gly**-Leu-Phe-Val-OMe. a = 9.883 Å, b = 12.238 Å, c = 46.861 Å	$P2_12_12_1$	4/1	Type II′	1 H_2O	Parallel	4*b*
8	Boc-Leu-Phe-Val-**^{D}Pro-Ala**-Leu-Phe-Val-OMe. a = 19.107 Å, b = 23.905 Å, c = 28.450 Å	$P2_12_12_1$	8/2	Type II′	3 H_2O + 1 isopropanol	Orthogonal	4*b*
9	Boc-Leu-Val-Val-**^{D}Pro-Aib**-Leu-Val-Val-OMe. a = 9.882 Å, b = 11.288 Å, c = 15.734 Å, α = 107.545°, β = 90.017°, γ = 104.261°	$P1$	1/1	Type II′	1 H_2O + 1 DMF	Parallel	4*b*
10	Boc-Met-Leu-Phe-Val-**^{D}Pro-Ala**-Leu-Val-Val-Phe-OMe. a = 12.153 Å, b = 24.100 Å, c = 27.990 Å, α = 101.02°, β = 102.51°, γ = 104.62°	$P1$	4/4	Type II′	4 H_2O	Antiparallel	4*b*
11	Boc-Leu-βPhe-Val-**^{D}Pro-Gly**-Leu-βPhe-Val-OMe. a = 19.555 Å, b = 11.352 Å, c = 28.912 Å, β = 101.909°	$P2_1$	4/2	Type II′	2 Ethanol	Parallel	29*f*
12	Boc-Leu-Phe-Val-**^{D}Pro-Ac6c**-Leu-Phe-Val-OMe. a = 18.143 Å, b = 24.858 Å, c = 18.449 Å, β = 117.02°	$P2_1$	4/2	Type II′	1 Dioxane + 1 H_2O	Orthogonal	8*a*
13	Boc-Leu-Phe-Val-**^{D}Pro-Ac8c**-Leu-Phe-Val-OMe. a = 15.039 Å, b = 25.900 Å, c = 19.083 Å, β = 108.498°	$P2_1$	4/2	Type II′	3 H_2O	Orthogonal	8*a*
14	Boc-Leu-Val-γAbu-Val-**^{D}Pro-Gly**-Leu-γAbu-Val-Val-OMe. a = 9.742 Å, b = 10.842 Å, c = 31.473 Å, α = 89.46°, β = 83.28°, γ = 78.85°	$P1$	2/2	Type II′	2 H_2O	Parallel	29*g*
15	Boc-Leu-Val-Val-**^{D}Pro-δAva**-Leu-Val-Val-OMe. a = 9.678 Å, b = 11.967 Å, c = 52.228 Å	$P2_12_12_1$	4/1	C_{13} ring	1 H_2O + 1 CH_3OH	Parallel	29*h*
16	Boc-Leu-Phe-Val-**Aib-Gpn**-Leu-Phe-Val-OMe. a = 9.558 Å, b = 26.278 Å, c = 27.434 Å	$P2_12_12_1$	4/1	C_{12} ring	1 Tetrahydrofuran (THF)	Parallel	29*i*
17	Boc-Leu-Phe-Val-**^{D}Pro-ψPro**-Leu-Phe-Val-OMe. a = 34.646 Å, b = 15.337 Å, c = 25.553 Å, β = 103.387°	$C2$	8/2	Type II′	3 H_2O	Orthogonal	29*j*
18	Boc-Leu-Val-Val-**Aib-^{D}Pro**-Leu-Val-Val-OMe. a = 11.0623 Å, b = 18.7635 Å, c = 16.6426 Å; β = 102.37°	$P2_1$	2/1	Type I′	2 DMF	Parallel	18
19	Boc-Leu-Phe-Val-**^{D}Pro-Pro**-Leu-Phe-Val-OMe (**1**) a = 14.4028 Å, b = 18.9623 Å, c = 25.4903 Å, β = 105.674°	$P2_1$	4/2	Type II′	1 H_2O	Orthogonal	Present study
20	Boc-Leu-Tyr-Val-**^{D}Pro-Pro**-Leu-Phe-Val-OMe (**2a**) a = 19.086 Å, b = 26.216 Å, c = 28.015 Å	$P2_12_12_1$	8/2	Type II′	3 H_2O	Orthogonal	Present study
21	Boc-Leu-Tyr-Val-**^{D}Pro-Pro**-Leu-Phe-Val-OMe (**2b**) a = 14.318 Å, b = 18.992 Å, c = 25.157 Å, β = 105.59°	$P2_1$	4/2	Type II′	3 H_2O	Orthogonal	Present study
22	Boc-Leu-Val-Val-**^{D}Pro-Pro**-Leu-Val-Val-OMe (**3**) a = 9.922 Å, b = 11.229 Å, c = 26.423 Å, α = 87.15°, β = 89.44°, γ = 73.28°	$P1$	2/2	Type II′	No solvent	Parallel	Present study
23	Boc-Leu-Phe-Val-**^{D}Pro-Aib**-Leu-Phe-Val-OMe (**4a**) a = 18.410 Å, b = 23.219 Å, c = 19.242 Å, β = 118.036°	$P2_1$	4/2	Type II′	1 H_2O + 1 dioxane	Orthogonal	Present study
24	Boc-Leu-Phe-Val-**^{D}Pro-Aib**-Leu-Phe-Val-OMe (**4b**) a = 18.095 Å, b = 23.031 Å, c = 18.637 Å, β = 117.471°	$P2_1$	4/2	Type II′	1 H_2O	Orthogonal	Present study
25	Boc-Leu-Phe-Val-**^{D}Pro-Ac6c**-Leu-Phe-Val-OMe (**5**) a = 18.880 Å, b = 24.579 Å, c = 28.780 Å	$P2_12_12_1$	8/2	Type II′	3 H_2O	Orthogonal	Present study
26	Boc-Leu-Phe-Val-**^{D}Pro-Ala**-Leu-Phe-Val-OMe (**6**) a = 19.042 Å, b = 23.627 Å, c = 28.591 Å	$P2_12_12_1$	8/2	Type II′	4 H_2O	Orthogonal	Present study

[a] Z: number of molecules in the unit cell; Z': number of molecules in the asymmetric unit.

Conclusions

The successful crystallization and study of a large number of model peptide hairpin sequences points towards a strategy for the creation of multi-stranded β-sheet structures.[26] So far, the trials to crystallize three and four stranded β-hairpins containing conformationally constrained ^{D}Pro-Xxx segments have not been successful. Designed β-hairpins constructed with predominantly apolar amino acids display high solubility in organic solvents and do not show a pronounced tendency to aggregate. The crystallographic studies on model β-hairpin peptide sequences and understanding the factors responsible for the growth of crystals and deciphering the interactions responsible for certain types of packing arrangements provides a first step in the design and construction of model polypeptide sequences that can fold into completely β-sheet structures. In addition, these motifs can also serve as templates to generate novel folds with a mixture of α-helical and β-hairpin fragments.[27] The observed packing modes for the β-strand segments may be of relevance in modeling multiple modes of association that may provide insights into the structure of insoluble polypeptide aggregates. A detailed understanding of the nucleation and growth of crystals of β-hairpin peptides will undoubtedly benefit from an analysis of the modes of peptide association in solution. While considerable efforts have been expended on conformational analysis in solution, peptide association in this class of molecules remains to be investigated.

Experimental section

Peptide synthesis

The peptides were synthesized by classical solution phase methods by using a racemization-free fragment condensation strategy. The *tert*-butyloxycarbonyl (Boc) group was used to protect the N-terminus. Deprotections were performed using 98% formic acid and saponification for the N- and C-terminal protection groups, respectively. Couplings were mediated by *N*,*N*′-dicyclohexylcarbodiimide (DCC) and 1-hydroxybenzotriazole (HOBt). All the intermediates were characterized by ^{1}H NMR (80 MHz) and TLC (silica gel, chloroform–methanol 9 : 1), and were used without further purification. The final peptides were purified by reverse phase, medium-pressure liquid chromatography (C_{18}) and high performance liquid chromatography (HPLC) on a reverse phase C_{18} column (5–10 μ, 7.8 × 250 mm) using methanol–water gradients. The purified peptides were characterized by electrospray or MALDI and 500 MHz ^{1}H NMR spectra (ESI Fig. S9 and S10†) (peptide **1**: MNa_{obs}^{+} = 1067, M_{calc} = 1044; peptide **2**: MNa_{obs}^{+} = 1083, M_{calc} = 1060; peptide **3**: MNa_{obs}^{+} = 971; M_{calc} = 948; peptide **4**: MNa_{obs}^{+} = 1055, M_{calc} = 1032; peptide **5**: MNa_{obs}^{+} = 1095, M_{calc} = 1072; peptide **6**: MNa_{obs}^{+} = 1041.7, M_{calc} = 1018.5).

X-ray diffraction

Single crystals suitable for X-ray diffraction were obtained by the slow evaporation of solutions of the peptides in a range of solvent conditions. Colorless single crystals for the peptides **1–3**

Table 2 Crystal and diffraction parameters for the peptides **1–3**

	1	2a	2b	3
Empirical formula	$C_{56}H_{84}N_8O_{11.5}$	$C_{56}H_{83}N_8O_{13.5}$	$C_{56}H_{83}N_8O_{13.5}$	$C_{48}H_{84}N_8O_{11}$
Crystal habit	Plates	Plates	Plates	Plates
Crystal size [mm]	0.80 × 0.12 × 0.01	0.40 × 0.20 × 0.04	0.49 × 0.09 × 0.05	0.49 × 0.09 × 0.05
Crystallizing solvent	Methanol–water	Methanol–water	Methanol–water	Methanol–water
Space group	$P2_1$	$P2_12_12_1$	$P2_1$	$P1$
a [Å]	14.403 (8)	19.086 (4)	14.318 (8)	9.922 (3)
b [Å]	18.962 (1)	26.216 (5)	18.992 (9)	11.229 (4)
c [Å]	25.490 (1)	28.015 (6)	25.157 (1)	26.423 (9)
α, β, γ [°]	105.67 (4)		105.59 (4)	87.15 (6), 89.44 (6), 73.28 (7)
Volume [Å^3]	6702.8 (7)	14 018.0 (5)	6589.5 (6)	2816.1 (1)
Z/Z'	4/2	8/2	4/2	2/2
Co-crystallized solvent	One water molecule	Three water molecules	Three water molecules	None
Molecular weight	1053.31	1084.81	1084.30	949.23
Density [g cm^{-3}] [calc.]	1.044	1.028	1.093	1.119
F (000)	2272	4668	2332	1032
Radiation	Cu K_α	Mo K_α	Cu K_α	Mo K_α
Temperature [°C]	21	21	21	21
θ Range [°]	3.60–71.83	1.55–20.18	1.82–71.74	1.54–23.26
Scan type	$\omega + \phi$	ω	$\omega + \phi$	ω
Measured reflections	33 680	14 663	34 052	27 419
Unique reflections	12 699	7212	12 393	8021
Observed reflections [$\|F\| > 4\sigma(F)$]	6142	2093	4214	2366
Final R [%]	9.59	9.89	12.49	10.58
Final wR_2 [%]	22.51	20.64	29.29	23.54
Goodness-of-fit (S)	0.925	1.032	1.075	0.932
$\Delta\rho_{max}/\Delta\rho_{min}$ [e Å^{-3}]	0.28/−0.21	0.32/−0.23	0.37/−0.27	0.37/−0.27
Restraints/parameters	4/1349	9/1351	4/1397	9/1202

Table 3 Crystal and diffraction parameters for the peptides **4–6**

	4a	**4b**	**5**	**6**
Empirical formula	$C_{57}H_{88}N_8O_{12.5}$	$C_{55}H_{84}N_8O_{11.5}$	$C_{58}H_{88}N_8O_{11}$	$C_{54}H_{78}N_8O_{12}$
Crystal habit	Plates	Plates	Plates	Needles
Crystal size [mm]	0.80 × 0.48 × 0.10	0.40 × 0.20 × 0.04	0.54 × 0.16 × 0.01	0.50 × 0.02 × 0.01
Crystallizing solvent	Dioxane–water	Dioxane–water	Methanol–water	DMF–water
Space group	$P2_1$	$P2_1$	$P2_12_12_1$	$P2_12_12_1$
a [Å]	18.410 (2)	18.095 (4)	18.880(3)	18.7511 (9)
b [Å]	23.220 (3)	23.032 (5)	24.579(4)	23.3396 (11)
c [Å]	19.240 (3)	18.637 (5)	28.780(5)	28.1926 (13)
α, β, γ [°]	118.06 (1)	117.47 (2)		
Volume [Å^3]	7260.0 (1)	6891.2 (3)	13 355(4)	12 338.3 (10)
Z/Z'	4/2	4/2	8/2	8/2
Co-crystallized solvent	One dioxane and one water molecule	One water molecule	Three water molecules	Two water molecules
Molecular weight	1085.35	1041.30	1099	1031.24
Density [g cm^{-3}] [calc.]	0.993	1.004	1.092	1.110
F (000)	2344	2248	4736	4432
Radiation	Mo K_α	Cu K_α	MoK_α	Cu K_α
Temperature [°C]	21	21	21	21
θ Range [°]	1.20–27.35	4.64–71.82	1.1–20.8	2.46–72.27
Scan type	ω	$\omega + \phi$	ω	$\omega + \phi$
Measured reflections	69 713	40 004	88 591	73 135
Unique reflections	13 869	12 050	7648	12 534
Observed reflections [$\|F\| > 4\sigma(F)$]	2772	4518	5737	3798
Final R [%]	10.12	9.15	12.49	12.08
Final wR_2 [%]	20.61	20.96	22.62	28.98
Goodness-of-fit (S)	0.865	0.985	0.961	1.041
$\Delta\rho_{max}/\Delta\rho_{min}$ [e Å^{-3}]	0.14/−0.14	0.40/−0.15	0.29/−0.25	0.36/−0.33
Restraints/parameters	11/1349	7/1343	0/1424	0/1334

and **5** were grown from methanol–water, **4** from dioxane–water, and **6** from DMF–water, respectively. Initially, all the X-ray diffraction data on the crystals of peptides **1–6** were collected on a Bruker AXS SMART APEX CCD diffractometer (equipped with sealed tube Mo K_α source, λ = 0.71073 Å). All the crystals were preserved. With the availability of a rotating-anode X-ray single crystal diffractometer equipped with intense CuK_α (λ = 1.54178 Å) radiation at the Indian Institute of Science, it was felt necessary to improve the data quality of all the crystals by a recollection of the diffraction data on a Bruker AXS ULTRA APEXII CCD diffractometer (rotating anode X-ray generator). It was found that only a few of the crystals retained crystallinity, as the time gap between the data recollection was approximately 2 years. The crystal of **2a** was decaying and had started growing whitish in color. The crystal did not diffract in the X-ray beam. The preserved crystals were checked for any crystal showing signs of crystallinity. It was observed that a few of the crystals retained signs of crystallinity under the polarizing microscope; the rest were no longer transparent. One of the crystals was picked to recollect the X-ray diffraction data. Surprisingly, the crystal could be unequivocally indexed in a cell corresponding to the monoclinic space group ($P2_1$), in contrast to the orthorhombic cell parameters in **2a**. It was clear that this was a new crystal form (**2b**) and the cell dimensions of **2b** corresponded closely to peptide **1**. Diffraction data was also collected on a new crystal of peptide **4a**; the earlier crystal had lost crystallinity and did not diffract in the X-ray beam. It was observed that the cell dimensions showed a small change from that of **4a**, concomitant with a significant change in cell volume, 7260 Å^3 in **4a** and 6891 Å^3 in **4b**. The X-ray diffraction data collected for the crystals **1–6** are summarized in Tables 2 and 3. The structures of all the octapeptide sequences **1–6** were solved by direct methods using SHELXD,[28] which combines 'peak list optimization' with the 'minimal function' involving dual space recycling. All the structures were observed to have two molecules in the asymmetric unit. The structures were refined against F^2, with full-matrix least squares methods by using SHELXL-97[28] for peptides **1**, **2b**, **4a**, **4b**, **5** and **6**, and the two molecules were treated as two separate blocks in the case of peptides **2a** and **3**. The final values after the refinement of crystal structures are shown in Tables 1 and 2. CCDC 821276 (**1**), 821280 (**2a**), 821281 (**2b**), 821277 (**3**), 821278 (**4a**), 821279 (**4b**), 821275 (**5**) and 821274 (**6**) contain the supplementary crystallographic data for this paper.

Acknowledgements

This research was supported by a grant from the Council of Scientific and Industrial Research (CSIR) and a program grant from the Department of Biotechnology, India, in the area of Molecular Diversity and Design, India. S.A. and V.V.H. thank the CSIR for a Research Associateship and a Senior Research Fellowship respectively. U.S.R. thanks the University Grants Commission for a Senior Research Fellowship.

References

1 (*a*) M. Balbirnie, R. Grothe and D. S. Eisenberg, *Proc. Natl. Acad. Sci. U. S. A.*, 2001, **98**, 2375; (*b*) R. Nelson,

M. R. Sawaya, M. Balbirnie, A. Ã. Madsen, C. Riekel, R. Grothe and D. Eisenberg, *Nature*, 2005, **435**, 773; (*c*) R. Nelson and D. Eisenberg, *Curr. Opin. Struct. Biol.*, 2006, **16**, 260; (*d*) R. Nelson and D. Eisenberg, *Adv. Protein Chem.*, 2006, **73**, 235.

2 (*a*) F. Chiti and C. M. Dobson, *Annu. Rev. Biochem.*, 2006, **75**, 333; (*b*) D. Eisenberg, R. Nelson, M. R. Sawaya, M. Balbirnie, S. Sambashivan, M. I. Ivanova, A. Ã. Madsen and C. Riekel, *Acc. Chem. Res.*, 2006, **39**, 568.

3 (*a*) O. Khakshoor, A. J. Lin, T. P. Korman, M. R. Sawaya, S. C. Tsai, D. Eisenberg and J. S. Nowick, *J. Am. Chem. Soc.*, 2010, **132**, 11622; (*b*) C. Liu, M. R. Sawaya, P. N. Cheng, J. Zheng, J. S. Nowick and D. Eisenberg, *J. Am. Chem. Soc.*, 2011, **133**, 6736; (*c*) P. Hoogerhout, W. Kamphuis, H. F. Brugghe, J. A. Sluijs, H. A. M. Timmermans, J. Westdijk, G. Zomer, C. J. P. Boog, E. M. Hol and G. P. J. M. van den Dobbelsteen, *PLoS One*, 2011, **6**(4), e19110, DOI: 10.1371/journal.pone.0019110.

4 (*a*) J. Venkatraman, S. C. Shankaramma and P. Balaram, *Chem. Rev.*, 2001, **101**, 3131; (*b*) S. Aravinda, V. V. Harini, N. Shamala, C. Das and P. Balaram, *Biochemistry*, 2004, **43**, 1832.

5 (*a*) M. López de la Paz, K. Goldie, J. Zurdo, E. Lacroix, C. M. Dobson, A. Hoenger and L. Serrano, *Proc. Natl. Acad. Sci. U. S. A.*, 2002, **99**, 16052; (*b*) A. Esteras-Chopo, M. T. Pastor and M. López de la Paz, *Methods Mol. Biol.*, 2006, **340**, 253; (*c*) B. L. Kagan, *Adv. Exp. Med. Biol.*, 2010, **677**, 150.

6 (*a*) C. M. Venkatachalam, *Biopolymers*, 1968, **6**, 1425; (*b*) G. D. Rose, L. M. Gierasch and J. A. Smith, *Adv. Protein Chem.*, 1985, **37**, 1; (*c*) J. S. Richardson and D. C. Richardson, in *Prediction of Protein Structure and the Principles of Protein Conformation*, ed. G. D. Fasman, Plenum Press, New York, 1989, pp. 1–98; (*d*) C. M. Wilmot and J. M. Thornton, *J. Mol. Biol.*, 1988, **203**, 221.

7 (*a*) S. K. Awasthi, S. Raghothama and P. Balaram, *Biochem. Biophys. Res. Commun.*, 1995, **216**, 375; (*b*) T. S. Haque, J. C. Little and S. H. Gellman, *J. Am. Chem. Soc.*, 1996, **118**, 6975; (*c*) T. S. Haque and S. H. Gellman, *J. Am. Chem. Soc.*, 1997, **119**, 2303; (*d*) S. R. Raghothama, S. K. Awasthi and P. Balaram, *J. Chem. Soc., Perkin Trans. 2*, 1998, 137; (*e*) H. L. Schenck and S. H. Gellman, *J. Am. Chem. Soc.*, 1998, **120**, 4869; (*f*) J. F. Espinosa and S. H. Gellman, *Angew. Chem., Int. Ed.*, 2000, **39**, 2330.

8 (*a*) V. V. Harini, S. Aravinda, R. Rai, N. Shamala and P. Balaram, *Chem.–Eur. J.*, 2005, **11**, 3609; (*b*) R. Bardi, A. M. Piazzesi, C. Toniolo, M. Sukumar, P. Antony Raj and P. Balaram, *Int. J. Pept. Protein Res.*, 1985, **25**, 628; (*c*) P. K. C. Paul, M. Sukumar, R. Bardi, A. M. Piazzesi, G. Valle, C. Toniolo and P. Balaram, *J. Am. Chem. Soc.*, 1986, **108**, 6363; (*d*) G. Valle, M. Crisma, C. Toniolo, N. Sen, M. Sukumar and P. Balaram, *J. Chem. Soc., Perkin Trans. 2*, 1987, 393; (*e*) A. Crisma, M. Bonora, G. M. Sonara and C. Toniolo, *Macromolecules*, 1988, **21**, 2064.

9 C. M. K. Nair, M. Vijayan, Y. V. Venkatachalapathi and P. Balaram, *J. Chem. Soc., Chem. Commun.*, 1979, 1183.

10 (*a*) J. A. Robinson, *Synlett*, 1999, 429; (*b*) J. A. Robinson, *Acc. Chem. Res.*, 2008, **41**, 1278; (*c*) J. A. Robinson, S. Demarco, F. Gombert, K. Moehle and D. Obrecht, *Drug Discovery Today*, 2008, **13**, 944.

11 J. A. Robinson, *Curr. Opin. Chem. Biol.*, 2011, **15**, 379.

12 J. A. Robinson, S. C. Shankaramma, P. Jetter, U. Kienzl, R. A. Schwendener, J. W. Vrijbloed and D. Obrecht, *Bioorg. Med. Chem.*, 2005, **13**, 2055.

13 N. Srinivas, P. Jetter, B. J. Ueberbacher, M. Werneburg, K. Zerbe, J. Steinmann, B. Van der Meijden, F. Bernardini, A. Lederer, R. L. A. Dias, P. E. Misson, H. Henze, J. Zumbrunn, F. O. Gombert, D. Obrecht, P. Hunziker, S. Schauer, U. Ziegler, A. Käch, L. Eberl, K. Riedel, S. J. DeMarco and J. A. Robinson, *Science*, 2010, **327**, 1010.

14 (*a*) R. V. Rughani and J. P. Schneider, *MRS Bull.*, 2008, **33**, 530; (*b*) K. Rajagopal, M. S. Lamm, L. A. Haines-Butterick, D. J. Pochan and J. P. Schneider, *Biomacromolecules*, 2009, **10**, 2619; (*c*) M. Gungormus, M. Branco, H. Fong, J. P. Schneider, C. Tamerler and M. Sarikaya, *Biomaterials*, 2010, **31**, 7266; (*d*) A. Altunbas, S. J. Lee, S. A. Rajasekaran, J. P. Schneider and D. J. Pochan, *Biomaterials*, 2011, **32**, 5906.

15 R. Rai, S. Raghothama and P. Balaram, *J. Am. Chem. Soc.*, 2006, **128**, 2675.

16 (*a*) G. R. Marshall and H. E. Bosshard, *Circ. Res.*, 1972, **30**/**31**(Suppl. II), 143; (*b*) A. W. Burgess and S. J. Leach, *Biopolymers*, 1973, **12**, 2599; (*c*) N. Shamala, R. Nagaraj and P. Balaram, *Biochem. Biophys. Res. Commun.*, 1977, **79**, 292; (*d*) N. Shamala, R. Nagaraj and P. Balaram, *J. Chem. Soc., Chem. Commun.*, 1978, 996; (*e*) R. Nagaraj, N. Shamala and P. Balaram, *J. Am. Chem. Soc.*, 1979, **101**, 16; (*f*) I. L. Karle and P. Balaram, *Biochemistry*, 1990, **29**, 6747; (*g*) C. Toniolo and E. Benedetti, *Trends Biochem. Sci.*, 1991, **16**, 350; (*h*) E. Benedetti, *Biopolymers*, 1996, **40**, 3.

17 S. Aravinda, N. Shamala, R. Rajkishore, H. N. Gopi and P. Balaram, *Angew. Chem., Int. Ed.*, 2002, **41**, 3863.

18 U. S. Raghavender, S. Aravinda, R. Rai, N. Shamala and P. Balaram, *Org. Biomol. Chem.*, 2010, **8**, 3133.

19 (*a*) G. Némethy and M. P. Printz, *Macromolecules*, 1972, **5**, 755; (*b*) E. J. Milner-White, B. M. Ross, R. Ismail, K. Belhady-Mostafa and R. Poet, *J. Mol. Biol.*, 1988, **204**, 777; (*c*) E. J. Milner-White, *J. Mol. Biol.*, 1990, **216**, 386.

20 (*a*) G. N. Ramachandran, A. V. Lakshminarayanan, R. Balasubramanian and G. Tegoni, *Biochim. Biophys. Acta, Protein Struct.*, 1970, **221**, 165; (*b*) T. Ashida and M. Kakudo, *Bull. Chem. Soc. Jpn.*, 1974, **47**, 1129; (*c*) D. F. De Tar and N. P. Luthra, *J. Am. Chem. Soc.*, 1977, **99**, 1232.

21 (*a*) S. K. Burley and G. A. Petsko, *Adv. Protein Chem.*, 1988, **39**, 125; (*b*) M. L. Waters, *Curr. Opin. Chem. Biol.*, 2002, **6**, 736; (*c*) R. M. Hughes and M. L. Waters, *Curr. Opin. Struct. Biol.*, 2006, **16**, 514; (*d*) J. B. O. Mitchell, R. A. Laskowski and J. M. Thornton, *Proteins: Struct., Funct., Genet.*, 1997, **29**, 370; (*e*) G. B. McGaughey, M. Gagnes and A. K. Rappe, *J. Biol. Chem.*, 1998, **273**, 15458; (*f*) S. Aravinda,

N. Shamala, C. Das, A. Sriranjini, I. L. Karle and P. Balaram, *J. Am. Chem. Soc.*, 2003, **125**, 5308.

22 G. D. Rose, W. B. Young and L. M. Gierasch, *Nature*, 1983, **304**, 654.

23 (*a*) C. Toniolo and E. Benedetti, *Macromolecules*, 1991, **24**, 4004; (*b*) I. L. Karle, *Acta Crystallogr., Sect. B: Struct. Sci.*, 1992, **48**, 341; (*c*) S. Aravinda, N. Shamala, R. S. Roy and P. Balaram, *Proc.–Indian Acad. Sci., Chem. Sci.*, 2003, **115**, 373; (*d*) C. Toniolo, M. Crisma, F. Formaggio, C. Peggion, Q. B. Broxterman and B. Kaptein, *Biopolymers*, 2004, **76**, 162; (*e*) M. Crisma, F. Formaggio, A. Moretto and C. Toniolo, *Biopolymers*, 2006, **84**, 3; (*f*) S. Aravinda, N. Shamala and P. Balaram, *Chem. Biodiversity*, 2008, **5**, 1238.

24 P. G. Vasudev, N. Shamala and P. Balaram, *J. Phys. Chem.*, 2008, **112**, 1308.

25 P. Chakrabarti and S. Chakrabarti, *J. Mol. Biol.*, 1998, **284**, 867.

26 (*a*) C. Das, S. Raghothama and P. Balaram, *J. Am. Chem. Soc.*, 1998, **120**, 5812; (*b*) J. Venkatraman, G. A. Naganagowda and P. Balaram, *J. Am. Chem. Soc.*, 2002, **124**, 4987.

27 I. L. Karle, C. Das and P. Balaram, *Proc. Natl. Acad. Sci. U. S. A.*, 2000, **97**, 3034.

28 G. M. Sheldrick, *Acta Crystallogr., Sect. A: Found. Crystallogr.*, 2008, **64**, 112.

29 (*a*) I. L. Karle, S. K. Awasthi and P. Balaram, *Proc. Natl. Acad. Sci. U. S. A.*, 1996, **93**, 8189; (*b*) C. Das, G. A. Naganagowda, I. L. Karle and P. Balaram, *Biopolymers*, 2001, **58**, 335; (*c*) I. L. Karle, H. N. Gopi and P. Balaram, *Proc. Natl. Acad. Sci. U. S. A.*, 2001, **98**, 3716; (*d*) I. L. Karle, H. N. Gopi and P. Balaram, *Proc. Natl. Acad. Sci. U. S. A.*, 2002, **99**, 5160; (*e*) H. N. Gopi, R. S. Roy, S. Raghothama, I. L. Karle and P. Balaram, *Helv. Chim. Acta*, 2002, **85**, 3313; (*f*) R. S. Roy, H. N. Gopi, S. Raghothama, R. D. Gilardi, I. L. Karle and P. Balaram, *Biopolymers*, 2005, **80**, 787; (*g*) R. S. Roy, H. N. Gopi, S. Raghothama, I. L. Karle and P. Balaram, *Chem.–Eur. J.*, 2006, **12**, 3295; (*h*) R. Rai, P. G. Vasudev, K. Ananda, S. Raghothama, N. Shamala, I. L. Karle and P. Balaram, *Chem.–Eur. J.*, 2007, **13**, 5917; (*i*) S. Chatterjee, P. G. Vasudev, S. Raghothama, C. Ramakrishnan, N. Shamala and P. Balaram, *J. Am. Chem. Soc.*, 2009, **131**, 5956; (*j*) Kantharaju, S. Raghothama, U. S. Raghavender, S. Aravinda, N. Shamala and P. Balaram, *Biopolymers*, 2009, **92**, 405.

